Clim Dyn (2012) 39:1661–1671
DOI 10.1007/s00382-011-1257-0

# Low-frequency modulation of the Atlantic warm pool by the Atlantic multidecadal oscillation

**Liping Zhang · Chunzai Wang · Lixin Wu**

Received: 4 June 2011 / Accepted: 23 November 2011 / Published online: 6 December 2011


**Abstract** This paper investigates the low-frequency modulation of the Atlantic warm pool (AWP) by the Atlantic multidecadal oscillation (AMO). Consistent with previous study, it shows that the time series of AWP area varies in phase with the AMO on multidecadal timescales. However, the variability of AWP area is out of phase with the AMO: A small (large) variance of AWP area is associated with the AMO warm (cold) phase. In addition, the modulation of AWP area variability by the AMO has a large seasonality, with a small (large) modulation in summer (fall). The modulation of the annual AWP area variability is primarily determined by the low frequency changes in the Pacific ENSO and the local heat flux feedback, and countered by the low frequency changes in the North Atlantic Oscillation and the ocean mixed layer depth. The local heat flux feedback and mixed layer depth change also play important roles in the AMO-modulated seasonality of the AWP area variability.

**Keywords** Atlantic warm pool · Atlantic multidecadal oscillation · Low-frequency variability

## 1 Introduction

The Atlantic warm pool (AWP) is a large body of warm water in the low latitudes of the North Atlantic, which comprises the Gulf of Mexico, the Caribbean Sea, and the western tropical North Atlantic (Wang and Enfield 2001, 2003). As the second largest body of warm water on the earth, the AWP hosts the second largest diabatic heating center in the boreal summer Tropics. The AWP has a large seasonal cycle, and its area shows large fluctuations, with large warm pools being almost three times larger than small ones (Wang et al. 2006). Previous studies have shown that atmospheric circulation exhibits significant differences in response to large AWP and small AWP (Wang et al. 2008a, b). In addition to the seasonal cycle of the AWP area, Wang et al. (2008b) further pointed out that the AWP area variability occurs on both interannual and multidecadal timescales as well as with a long term warming trend.

In general, large (small) AWP areas coincide with anomalous warming (cooling) of the tropical North Atlantic region (Enfield et al. 2006). Interannual variability of the tropical North Atlantic SST is suggested to be associated with the Pacific El Niño-Southern Oscillation (ENSO) and the North Atlantic Oscillation (NAO) (e.g., Enfield and Mayer 1997; Klein et al. 1999; Hastenrath 2000; Giannini et al. 2001; Czaja et al. 2002; Nigam 2003), both of which have significant teleconnections to the tropical North Atlantic. As expected, the AWP area fluctuates with the ENSO and NAO accordingly (Enfield et al. 2006). There is a general agreement that the ENSO-induced tropical Atlantic SST and AWP area fluctuations result from a varied downward heat flux, including latent heat flux due to changes in the strength of the trade wind (Curtis and Hastenrath 1995; Giannini et al. 2000; Enfield et al. 2006) or the amount of moisture (Saravanan and Chang 2000), and radiative flux as a result of cloud changes (Klein et al. 1999). There are several atmospheric pathways that can bridge the Pacific ENSO with the North Atlantic

L. Zhang · L. Wu (✉)
Physical Oceanography Laboratory, Ocean University of China, Qingdao, China
e-mail: lxwu@ouc.edu.cn

C. Wang
NOAA Atlantic Oceanographic and Meteorological Laboratory, 4301 Rickenbacker Causeway, Miami, FL 33149, USA

surface variations. Hastenrath (2000) attributed the connection to the Rossby wave propagation (Hoskins and Karoly 1981) which is commonly known as the Pacific North American teleconnection (Horel and Wallance 1981). Alternatively, Wang (2002) and Wang and Enfield (2003) presented evidence that the North Atlantic variability is consistent with ENSO-induced anomalous divergent (Walker–Hadley) circulation. On the other hand, the influence of the NAO on tropical Atlantic SST is quite clear, which is primarily through its southern node that encompasses the subtropical pressure system and has the great potential to affect the associated northeast trade wind (Czaja et al. 2002). In addition to the external forcings, interannual variability of tropical North Atlantic SST (or AWP area) can also be influenced by local forcings: local ocean–atmosphere interaction (Xie and Philander 1994) and/or ocean mixed layer depth change.

The multidecadal variability of the AWP area is found to vary in phase with the Atlantic multidecadal oscillation (AMO) (Wang et al. 2008b). The AMO, which can be defined as the first rotated empirical orthogonal function (EOF) of the non-ENSO global SST (Enfield and Mestas-Nuñez 1999; Mestas-Nuñez and Enfield 1999), is the strongest multidecadal modes in the Atlantic Ocean. Many regional phenomena have been found to link with the AMO, such as the Northeast Brazilian and African Sahel rainfall (Folland et al. 1986; Rowell et al. 1995; Folland et al. 2001; Rowell 2003), Atlantic hurricanes (Goldenberg et al. 2001) and North American and European summer climate (Enfield et al. 2001; McCabe et al. 2004; Sutton and Hodson 2005). In spite of its importance, the mechanism of the AMO is still unclear. One of the most popular arguments is that the AMO is induced by the Atlantic thermohaline circulation variations and associated heat transport fluctuations (Folland et al. 1986; Gray et al. 1997; Delworth and Mann 2000; Knight et al. 2005). The coincidence of multidecadal phase between the AWP and AMO suggests that the slowly evolving AMO with a period of multidecadal timescales (Schlesinger and Ramankutty 1994; Kerr 2000) may modulate the AWP shorter-term variability.

In this paper, we attempt to examine the modulation of the AWP area variability by the AMO and to provide the possible interpretations. The paper is organized as follows. Section 2 briefly presents the data sets that we have used. The AMO's modulation on the AWP area variance is shown in Sect. 3. The mechanisms to explain the AMO's modulation on the AWP area variance, the roles of ENSO and NAO teleconnections as well as local impacts are proposed and examined in Sect. 4. Section 5 investigates the ENSO and NAO teleconnections to the tropical North Atlantic during the AMO warm and cold phases. The paper is concluded with a summary and some discussions.

## 2 Data sets

Several data sets are used in this study. The first one is the Hadley Center Sea Ice and Sea Surface Temperature (HadISST) data set (Rayner et al. 2003). The data is monthly and has a spatial resolution of 1° (latitude) ×1° (longitude). The length of the data spans from 1870 to 2010. The second data set is an improved extended reconstructed SST (ERSST), with a 2° latitude by 2° longitude resolution spanning from January 1854 to December 2006 (Smith and Reynolds 2004).

The corresponding long-term ocean subsurface temperature is taken from the new SODA reanalysis product, which is based on the Parallel Ocean Program (POP) ocean model with an average horizontal resolution of 0.5° × 0.5° and with 40 vertical levels. The temperature and salinity profile data, including the recent release of the World Ocean Database 2009 (WOD09), are assimilated. The assimilation of temperature and salinity observations is carried out sequentially using a 10-day updated cycle with model error covariance determined from a simulation that does not include assimilation. The ocean model surface boundary conditions are taken from a new atmospheric data set designated as 20CRv2 (twentieth century Reanalysis version 2), which contains the synoptic-observation-based estimate of global tropospheric variability spanning 1871–2008 at 6-hourly temporal and 2° spatial resolutions, and is derived using only observations of synoptic surface pressure and prescribing monthly SST and sea-ice distributions as boundary conditions for the atmosphere (Compo et al. 2011).

All variables are detrended before doing the analyses unless specified. When we calculate composites associated with the AMO, we focus on the period from 1900 to 1995 which encompasses 1.5 complete cycle of the AMO.

## 3 Modulation of AWP area variance by the AMO

The AWP area is calculated as the area of SST warmer than 28.5°C. Given that the AWP disappears during winter and early spring, the annual mean AWP area is only calculated from June to November. Consistent with the results in Wang et al. (2008b), annual mean AWP area varies on three major timescales: a secular trend, an interannual variation and a multidecadal variation (Fig. 1a, b). The secular trend indicates that the AWP becomes larger since the last century, in assoication with global warming. The multidecadal variability shows that the AWPs are large before 1890, during 1925–1965 and after 1995, and small during 1900–1924 and 1966–1994. As shown previously (Wang et al. 2008b), the AWP area multidecadal variability is in phase with the AMO—a mode operating primarily on

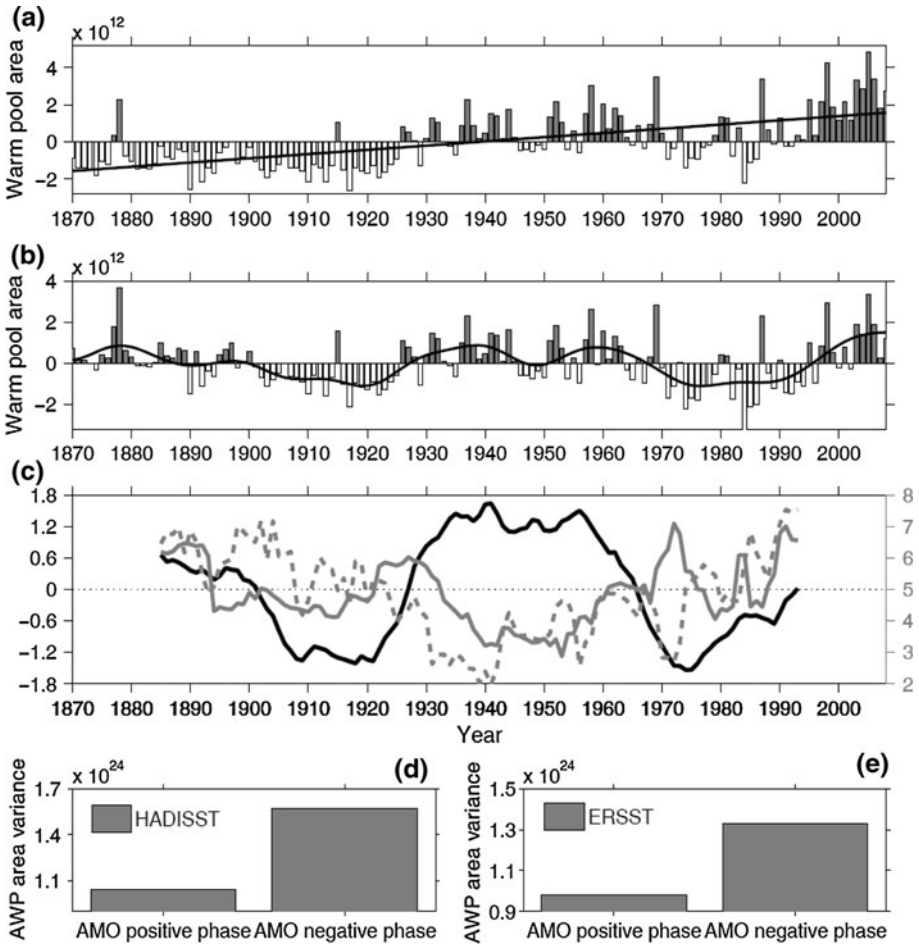


**Fig. 1** **a** Time series of Atlantic warm pool area anomaly during June–November in HADISST data. Unit is $m^2$. *Black line* superimposed denotes the trend in recent 139 years. **b** Detrended time series of (**a**), and *black curve* is obtained by performing a 7-year low frequency filter. **c** Time series of normalized AMO index (*black line*) defined as the the first rotated EOF of the non-ENSO global SST, normalized (divided by standard deviation) AWP area variance (*bold gray line*), and ENSO magnitude (*dash gray line*) (defined as standard deviation of the annual Niño3 index) in a running 31 year window based on the HADISST data. Note that similar results are obtained when ERSST data is used (not shown). **d** Composite analysis of AWP area variance in the AMO warm phase (1925–1965) and cold phases (1900–1924, 1966–1994), respectively based on the HadISST data set. **e** Same as (**d**) but using ERSST data

the North Atlantic. This is not surprising since the AWP locates entirely north of the equator. When the AMO is in its warm (cold) phase, warm (cold) SST anomaly occurs in the Northern Hemisphere accordingly, leading to a warmer (colder) SST around the warm pool, more (less) water warmer than 28.5°C and thus a larger (smaller) AWP.

Although the AWP area varies in phase with the AMO, its variance shows some differences. Figure 1c compares the AMO index with the detrended AWP area variance in a 31-year running window. The variance of AWP area shows a low-frequency variation with a large value from 1900 to 1932, followed by a low value from 1933 to 1968, and then a high value during 1970–1994. The small (large) AWP area variance coincides with the warm (cold) phase of the AMO, with a correlation coefficient of −0.58 (significant at 95% confidence level by *t* test and the effective degree of freedom is 10). In other words, the AWP area variance is smaller during the AMO warm phase (1925–1965) than that in the AMO cold phase (1900–1924, 1966–1994). A further calculation shows that the AWP area variance in the AMO cold phase (1900–1924, 1966–1994) is nearly 1.5 times as large as that in the AMO warm phase (1925–1965) (Fig. 1d, e) which is significant at 90% confidence level based on the *F* test. As shown later, different AWP variances during the AMO warm and cold phases induce different atmospheric responses both in pattern and magnitude.

The modulation of the AWP area variance by the AMO displays a distinct seasonality. Figure 2 displays monthly AWP area variance modulated by the AMO based on the HadISST and ERSST data sets, respectively. In general, the AMO exerts a more effective modulation on the AWP area variance in fall than in summer. The largest modulation occurs in September when the AWP area attains its maximum, with a small variance during the AMO warm phase and a large variance during the AMO cold phase. In June, August and November, the AWP variance during the AMO warm phase is slightly larger than that during the AMO cold phase. However, for the annual mean the cold (warm) phase of the AMO is associated with the large (small) AWP's variance, as shown in Fig. 1d, e.

## 4 Possible mechanisms

Several pathways have been proposed to affect tropical North Atlantic SST variability (Enfield et al. 2006). These

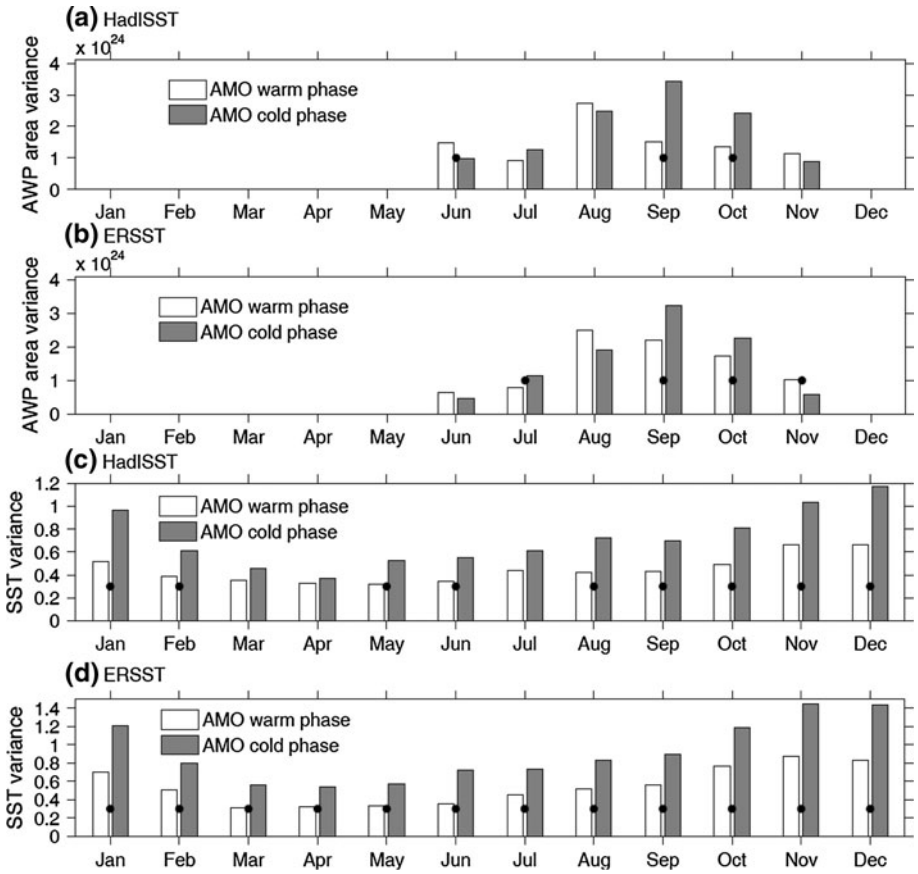


**Fig. 2** Seasonality of the AMO-modulated **a**, **b** AWP area variance and **c**, **d** SST amplitude based on HadISST and ERSST datasets, respectively. Units for (**a**, **b**) and (**c**, **d**) are $(m^2)^2$ and $(°C)^2$, respectively. *Black dots* indicate that the AWP area or SST variance difference between the AMO warm and cold phases is significant at 90% confidence level based on the *F* test

pathways include local influences such as the local ocean–atmosphere feedback (Xie and Philander 1994; Carton et al. 1996; Chang et al. 1997) and ocean mixed layer depth variation, and external forcing like ENSO (Covey and Hastenrath 1978; Hastenrath et al. 1984, 1987; Enfield and Mayer 1997; Klein et al. 1999; Giannini et al. 2000) and the NAO (Giannini et al. 2001; Mo and Häkkinen 2001; Czaja et al. 2002). Next, we examine factors by which the AMO can modulate the AWP area variance.

### 4.1 ENSO

The AMO can modulate ENSO which in turn influences the AWP. The modulation of ENSO in amplitude by the AMO is shown in Fig. 1c by calculating the Niño3 SST variance in a 31-year running window. Similar to the AWP area variance, the Niño3 SST variance varies out of phase with the AMO index. That is, a small (large) variance is associated with the warm (cold) phase of the AMO. The correlations of the Niño3 SST amplitude index with the AMO index and the AWP area variance are −0.68 and 0.7 (Fig. 1c), respectively (significant at 95% confidence level). AMO-modulated ENSO contribution to the AWP area variability is further revealed by the Wavelets of the Niño3 SST and AWP area index, which shows consistent results on interannual and decadal timescales with a small variance during the AMO warm phase and vice versa (Fig. 3c, d).

The difference of annually SST variance between the AMO warm phase (1925–1965) and cold phase (1966–1994, 1900–1924) is shown in Fig. 3a. The tropical North Atlantic region is characterized by a negative value, with a magnitude reaching to 0.025 $(°C)^2$. This indicates a weaker SST variability in the AMO warm phase than in the AMO cold phase. The tropical Pacific Ocean also shows large negative values, indicating a weak (strong) ENSO amplitude during the AMO warm (cold) phase.

Mechanisms of the multidecadal modulation of ENSO amplitude by the AMO have been studied by Dong et al. (2006) using the coupled model HadCM3. They demonstrated that the SST dipole over the Atlantic Ocean during the AMO warm (cold) phase could induce a deepened (shoaled) thermocline over the tropical Pacific and reduce (increase) the vertical stratification through atmospheric bridge, which in turn leads to a weakened (strengthened) ENSO amplitude. As shown in Fig. 3b, the tropical Pacific temperature difference (the AMO warm phase minus the AMO cold phase) is characterized by a warming anomaly in the thermocline (defined as the 20°C isotherm), with a strong warming in the west and a relatively weaker

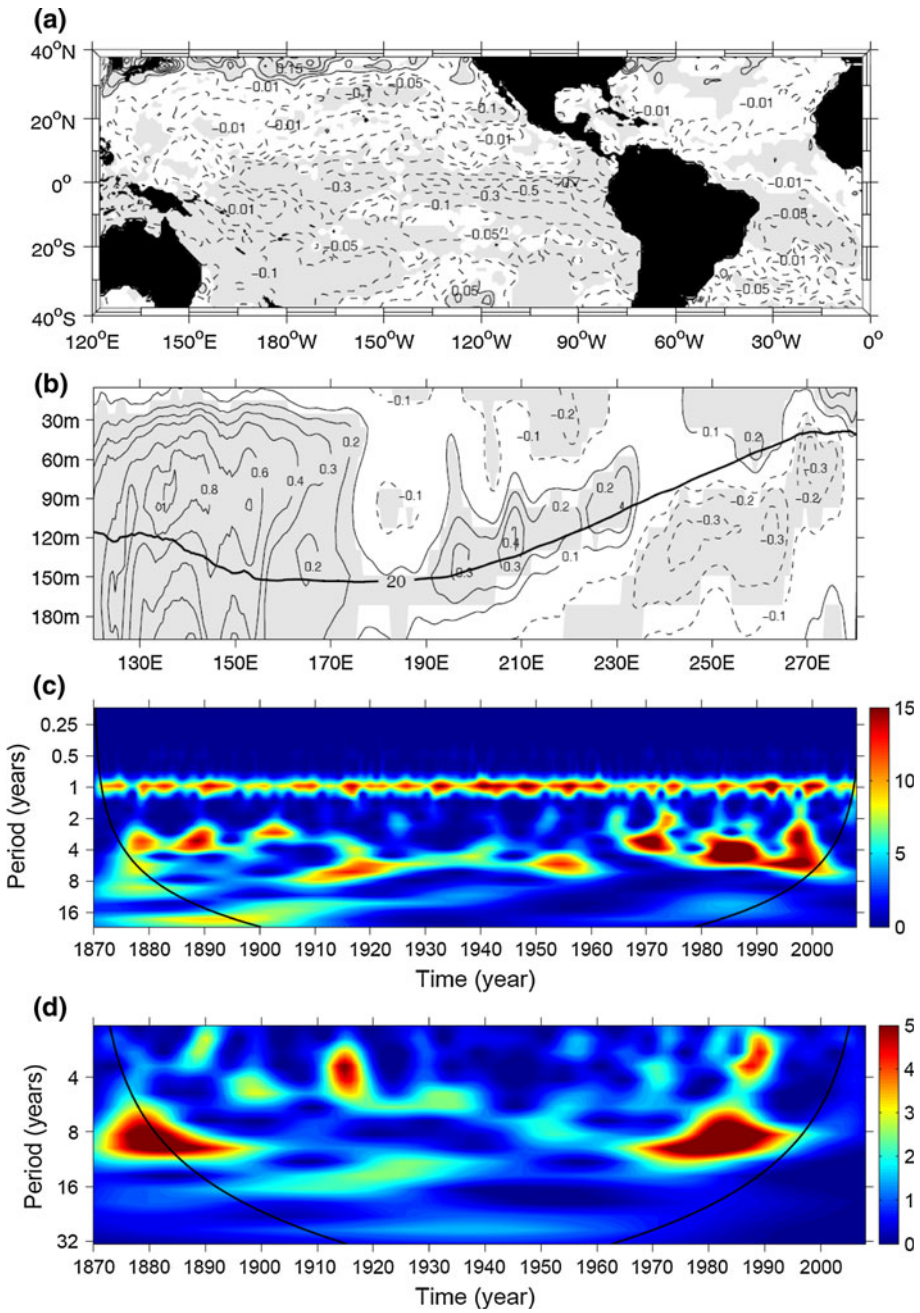


**Fig. 3** **a** Mean (June–November) SST variance difference in HadISST data calculated by subtracting the variance in the AMO cold phases (1966–1994, 1900–1924) from the variance in the AMO warm phase (1925–1965). Unit is $(°C)^2$. *Gray shaded* exceeds 90% confidence level based on the *F* test. **b** Differences in subsurface temperature (averaged between 10°S and 10°N) in the tropical Pacific Ocean (temperature in the AMO warm phase minus that in the AMO cold phase) using SODA data. Unit is °C. *Black line* superimposed depicts the climatological thermocline defined as the 20°C isotherm. *Gray shaded* exceeds 90% confidence level based on a Student's *t* test. **c** The wavelet power spectrum of Niño3 SST using the Morlet wavelet. The *left* axis is the period (in year). The *bottom* axis is time (in year). *Color shaded* indicates the total variance at a particular frequency explained at a particular time in the time series. The *black thick* contour encloses regions of greater than 90% confidence level for a white-noise process. **d** Same as (**c**) but for the AWP area index on interannual and decadal timescales

warming in the east. This thermal structure change implies a deep (shollow) thermocline over the tropical Pacific Ocean under the condition of the AMO warm (cold) phase. As the thermocline deepens, SST response to an anomaly in the thermocline depth should decrease, leading to a weakened ENSO amplitude, and vice versa.

On the other hand, it can be seen that AMO-modulated ENSO amplitude is also associated with the seasonal cycle (Fig. 3c). A close inspection finds that the seasonal cycle has a multidecadal oscillation, with a weak amplitude in the period of 1900–1924 and 1966–1998 and a strong amplitude in the period from 1925 to 1965. However, the amplitude of ENSO variability exhibits an opposite phase to the multidecadal variations of the seasonal cycle. Therefore, the AMO-modulated ENSO variability is also attributed to the seasonal cycle due to nonlinear interactions as proposed by Timmermann et al. (2007).

ENSO teleconnection to the tropical North Atlantic has been proposed by many studies primarily through corresponding atmospheric bridge and air–sea interaction (Enfield and Mayer 1997; Nigam 2003; Klein et al. 1999; Hastenrath 2000; Giannini et al. 2001; Czaja et al. 2002). Observations show that the tropical North Atlantic warming occurs during next spring following El Niño (Hastenrath

et al. 1987; Enfield and Mayer 1997). The ENSO-induced SST variation over the tropical North Atlantic is often suggested to be accompanied with changes of the North Atlantic subtropical high (Klein et al. 1999; Hastenrath 2000). As the subtropical high becomes strong or weak, wind in the southern branch changes accordingly and thus induces anomalous heat flux to cause SST fluctuations over the tropical North Atlantic. These are demonstrated in Fig. 4a, b by showing the wind speed and latent heat flux variance difference between the AMO warm and cold phases. The wind speed and flux changes correspond to a small SST variance in the tropical North Atlantic.

The multidecadal modulation of ENSO amplitude by the AMO has a seasonal dependence. As displayed in Fig. 2c, d, the AMO exerts the most effective modulation on ENSO during winter. In addition to winter, the AMO's modulation on the ENSO amplitude also occurs in other seasons. Nevertheless, ENSO teleconnection can not fully explain the seasonality of AWP area variance modulated by the AMO, since the AMO-modulated ENSO amplitude has a uniform response with a small variance during the AMO warm phase and a large variance during the AMO cold phase, whereas the opposite occurs for the AMO-modulated AWP area variance in summer. This implies that other mechanisms are existed to influence the AMO-modulated AWP area variance.

### 4.2 NAO

In addition to ENSO teleconnection, the tropical North Atlantic SST and AWP area variability are also influenced by the NAO (Grotzner et al. 1998; Czaja and Marshall 2001; Czaja et al. 2002; Enfield et al. 2006). The NAO is known to impact the trade winds and then SST anomalies over tropical North Atlantic through changes of surface turbulent heat flux (Halliwell and Mayer 1996; Carton et al. 1996). Here, we find that the AMO also exerts a multidecadal modulation on the NAO, which subsequently affects the AWP area variability. With regard to the short time delay of tropical North Atlantic response to the NAO (about 1 month) (Czaja et al. 2002), we focus on summer and fall when the AWP does appear. It can be seen that the NAO behaves oppositely in summer and fall. The NAO variance is smaller during the AMO warm phase than the AMO cold phase in summer, whereas the opposite is true in fall (Fig. 5). Meanwhile, the AMO-modulated effect on the NAO is quite larger in fall than that in summer, as revealed by the percentage change of NAO variance between the

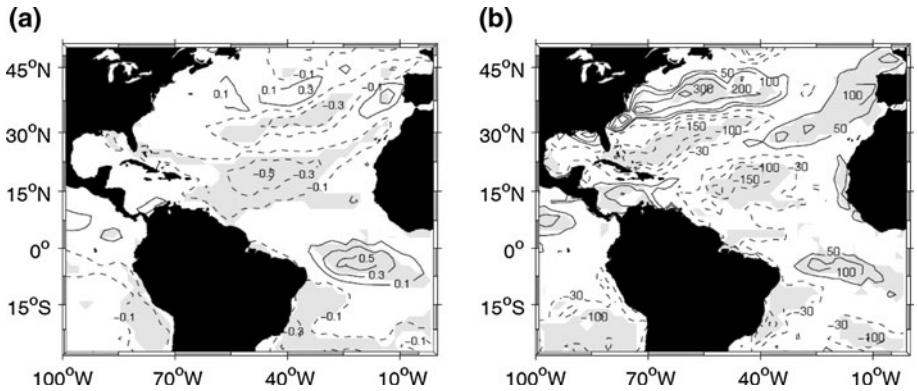


**Fig. 4** Same as Fig. 3a but for **a** wind speed variance at 10 m, and **b** latent heat flux variance at the surface. Data sets are from 20CRv2. Units for (**a**) and (**b**) are $(m/s)^2$ and $(W/m^2)^2$, respectively. *Gray shaded* exceeds 90% confidence level based on the *F* test

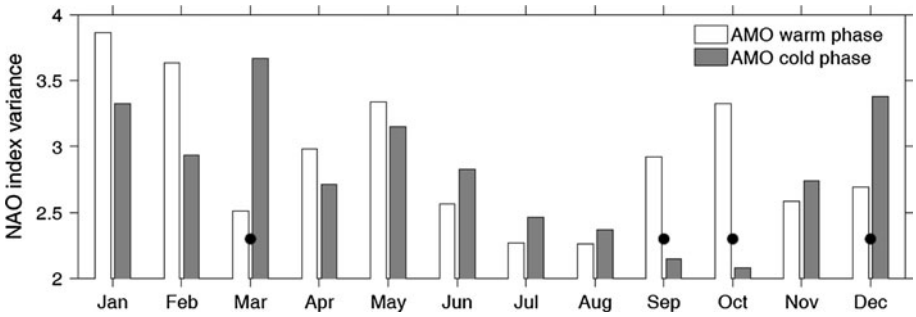


**Fig. 5** Same as Fig. 2c but for the NAO variance. The NAO index is downloaded from http://www.cgd.ucar.edu/cas/jhurrell/indices.data.html#naostatdjfm. *Black dots* indicate that NAO index variance difference between the AMO warm and cold phases at these months is significant at 90% confidence level based on the *F* test

AMO warm and cold phases. A further inspection finds that the NAO seasonality modulated by the AMO is countered by the seasonal fluctuations of the AWP area variance seen in Fig. 2 a, b, being indicative of a negative contribution of NAO teleconnection to the AWP area variance.

### 4.3 Ocean mixed layer depth

We first calculate the composites of the ocean mixed layer depth in the AMO warm and cold phases and we then obtain their differences (Fig. 6). The ocean mixed layer depth is defined as the depth where the difference with the potential density at the first layer equals to 0.125 kg/m$^3$. It is clearly seen that the mixed layer depth in the AWP region becomes shallower during the AMO warm phase compared to that during the AMO cold phase. This is largely due to the fact that tropical ocean mixed layer depth is primarily dominated by temperature. When the tropical North Atlantic is occupied by a warming SST anomaly during the AMO warm phase, the stratification is strengthened. As a result, sea water becomes more stable, and thus mixed layer depth shoals and vice versa.

As the ocean mixed layer depth shoals, SST response to an atmospheric forcing is enhanced. Thus, the mixed layer depth change modulated by the AMO should lead to a stronger AWP area variance in the AMO warm phase than that in the AMO cold phase. However, the annual AWP area displays a weak variability during the AMO warm phase (Fig. 1d, e), which counteracts the modulation effect of the mixed layer depth. Therefore, the local mixed layer depth change tends to weaken the annual AWP area variability modulated by the AMO. Additionally, it is worth noting that the amplitude of the mixed layer depth variance in summer is larger than that in fall (Fig. 6). This seasonal difference is in favor of generating a smaller AWP area variance during the AMO warm phase in fall than in summer and therefore tends to produce the modulation seasonality as shown in Fig. 2a, b.

### 4.4 Local air–sea coupling

It is difficult to determine the role of air–sea feedback over the tropical Atlantic from observations. The most classical theory involving wind, evaporation and SST (WES) is usually considered as a positive feedback to amplify SST anomaly north and south of the equator (Xie and Philander 1994; Chang et al. 2001). However, many studies show that the SST variations in the tropical South and North Atlantic are uncorrelated and that the dipole in the Inter-Tropical Covergence Cone (ITCZ) occur infrequently and no more than expected by chance (Houghton and Tourre 1992; Enfield and Mayer 1997; Enfield et al. 1999). Furthermore, Frankignoul and Kestenare (2002) pointed out that the heat flux feedback in the tropical Atlantic is negative based on the cross-covariance method. Here, we attempt to detect the changes of the heat flux feedback during the AMO phases.

Frankignoul and Kestenare (2002) use the cross-covariance method to estimate the strength of the heat flux feedback:

$$\alpha = -R_{TQ}(\tau)/-R_{TT}(\tau), \quad (1)$$

where $R_{TQ}$ is the cross-covariance of SST and net heat flux (positive downward), $R_{TT}$ is the auto-covariance of SST, and $\tau$ is the lag (when SST leads heat flux, $\tau < 0$). In view of the seasonality of the AWP area variance modulated by the AMO, the heat flux feedback is calculated in summer and fall, respectively. According to Frankignoul and Kestenare (2002), the seasonal dependence of the heat flux feedback was estimated with the lag of $-1$. To estimate $R_{TQ}(-1)$, summer was defined as June to September for Q and May to August for T, and fall by September to December for Q and August to November for T. The same was done for $R_{TT}(-1)$, with T instead of Q. Before calculating cross-covariance, all variables are detrended and the ENSO signal is removed by using the method of linear regression.

The heat flux feedback estimated from ERSST and 20CRv2 data is shown in Fig. 7. As expected, the climatological heat flux feedback is negative (positive value implies negative feedback) nearly everywhere in summer and fall, except some patches in the tropical North Atlantic (Fig. 7a, c). The net heat flux feedback is more negative at middle latitudes during fall than that in summer (Fig. 7a, c), which is primarily associated with turbulent heat flux component (not shown) due to a larger wind speed in fall.

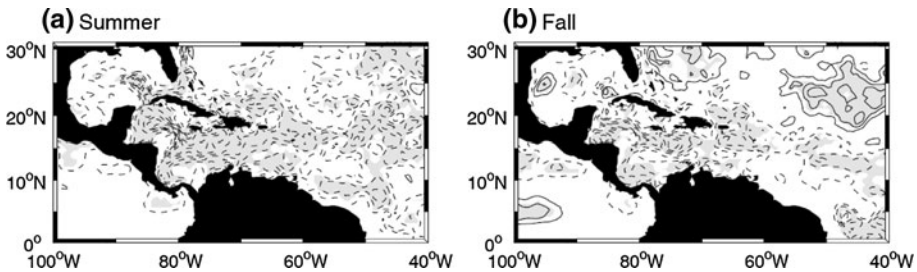


**Fig. 6** Differences in ocean mixed layer depth between the AMO warm phase and AMO cold phase in summer (JJA) and fall (SON), respectively. Unit is m. The SODA reanalysis data is used. Contour interval is 2 m. *Gray shaded* exceeds 90% confidence level based on the *t* test

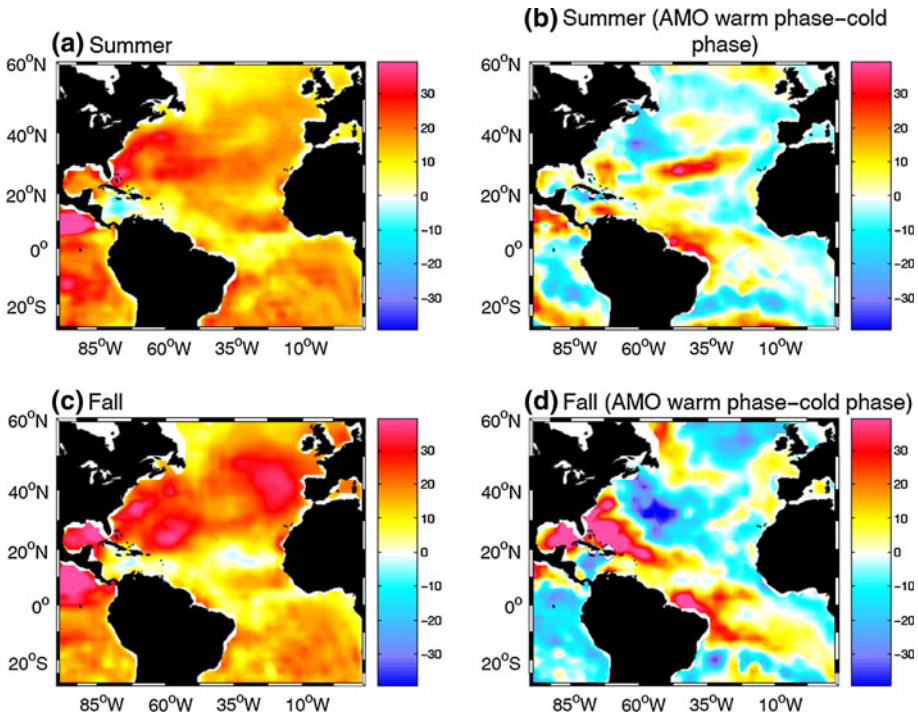


**Fig. 7** Climatological surface heat flux feedback in **a** summer and **c** fall. Unit is W/m$^2$/K. Positive value implies negative heat flux feedback. Heat flux feedback difference between the AMO warm phase and AMO cold phase in **b** summer and **d** fall. Unit is W/m$^2$/K

During the AMO warm phase, the negative heat flux feedback tends to strengthen in the tropical North Atlantic, but with larger amplitude in fall (Fig. 7b, d). The strengthened negative heat flux feedback over the AWP region during the AMO warm phase leads to a weakened SST variability, which in turn generates a small AWP area variance. Therefore, the local heat flux feedback in the AWP region plays an important role in observed annually AWP area variance fluctuations modulated by the AMO (as shown in Fig. 1d, e). Meanwhile, the local heat flux feedback can explain the seasonality of the AMO-modulated AWP area variance (Fig. 2a, b). As seen in Fig. 7b, d, the negative heat flux feedback difference in the AWP region in fall is larger than that in summer. This can explain the seasonality of the AWP area variance modulated by the AMO as shown in Fig. 2a, b.

## 5 Sensitivity of ENSO and NAO teleconnections to tropical North Atlantic during the AMO phases

Section 4 showed that the low-frequency modulation of the AWP area variance by the AMO is largely associated with ENSO, whereas the NAO contributes negatively. ENSO amplitude is weaker during the AMO warm phase than that during the AMO cold phase, which in turn can teleconnect to the tropical North Atlantic and modulate the AWP area variance. On the other hand, the seasonal changes of NAO amplitude modulated by the AMO appears to be less signficanlty. However, the annual mean (June–November) NAO amplitude is quite larger during the AMO warm phase than that during the AMO cold phase. This implies the AWP area variability modulated by the AMO is encountered by the NAO teleconnection. Here we investigate the sensitivity of ENSO and NAO teleconnections to the tropical North Atlantic by regressing Atlantic SST against the normalized ENSO and NAO indices during different AMO phases. With regard to the delay response of the tropical North Atlantic to external forcings, the Atlantic SST lags the ENSO and NAO indices by 4 months and 1 month, respectively.

Consistent with Enfield and Mayer (1997), the tropical Atlantic SST is well correlated with ENSO, with the Atlantic warming occurring 4 months after the mature phase of ENSO and vice versa (Fig. 8a, b). A close inspection finds that the warming magnitude of the tropical North Atlantic can reach to 0.16°C when the Niño3 SST has a unit standard deviation during the AMO warm phase and the associated pattern exhibits a northeast–southwest tilt (Fig. 8a). In the tropical South Atlantic, SST response synchronizes with the northern part but with a narrow range (Fig. 8a). In comparison with ENSO teleconnection in the AMO warm phase, tropical North Atlantic response to ENSO during the AMO cold phase displays a comparable magnitude but with a more flat west–east pattern (Fig. 8b). The difference of ENSO teleconnection to the Atlantic between the AMO warm and cold phases is shown in Fig. 8c, showing a negligible difference in magnitudes particularly in the western tropical North Atlantic. This implies that ENSO teleconnection to the tropical North

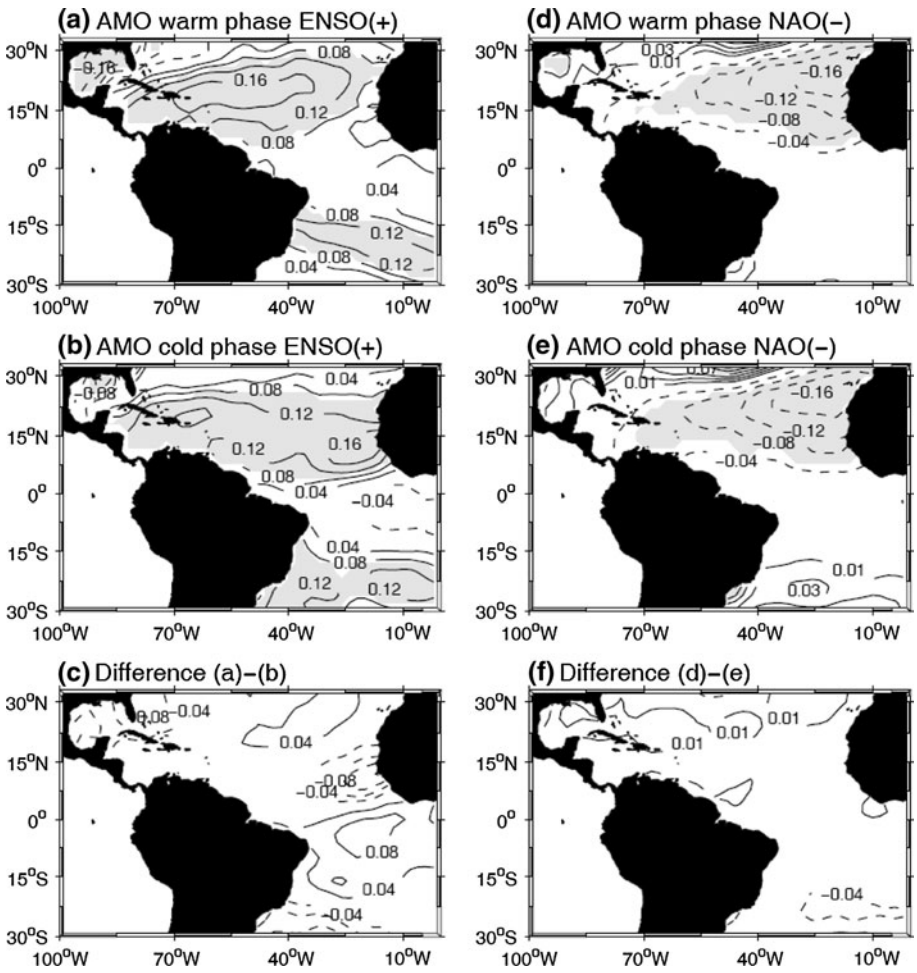


**Fig. 8** Regression of monthly SST against the normalized Niño3 SST index during **a** the AMO warm phase and **b** the AMO cold phase. The Niño3 SST leads Atlantic SST by 4 months. **c** Differences between (**a**) and (**b**). **d**, **e**, **f** is the same as (**a**, **b**, **c**) but for SST regression on the normalized NAO index. The Atlantic SST lags the NAO index by 1 month. Units for (**a**–**f**) are °C. *Gray shaded* exceeds 90% confidence level based on the *F* test

Atlantic during the AMO warm and cold phase is comparable. Thus, the AMO-modulated AWP area variability primarily depends on the amplitude of ENSO. The larger amplitude ENSO has, the larger AWP area variance is.

Similarly, the NAO teleconnection to the tropical North Atlantic also exerts a comparable response during the AMO warm and cold phases (Fig. 8d–f). As displayed in Fig. 8d, the tropical North Atlantic is characterized by a cold anomaly when the NAO is in its positive phase, consistent with previous studies (Giannini et al. 2001; Mo and Häkkinen 2001; Enfield et al. 2006). During both the AMO warm and cold phases, the tropical North Atlantic SST response can attain 0.16°C over the eastern tropical North Atlantic as the NAO varies with one standard deviation. The comparable NAO teleconnections during the AMO warm and cold phases is clearly displayed in Fig. 8e, which shows a negligible difference during the two AMO phases.

## 6 Discussion and summary

In this paper, the low-frequency modulation of the AWP area variability by the AMO is studied based on the combination of long-term observations and reanalysis products. Consistent with previous study of Wang et al. (2008b), it is shown that the AWP area displays multi-timescale variability: interannual, multidecadal variability and secular trend. On multidecadal timescales, the time series of the AWP area is in phase with the AMO, while its variance varies out of phase with the AMO. That is, a small (large) variance of the AWP area is associated with the AMO warm (cold) phase. Composite analyses further confirm this multidecadal modulation of the AWP area variance and show that the AWP area variance during the AMO cold phase is 1.5 times as large as that during the AMO warm phase. In addition, the AMO-modulated AWP area variance has a large seasonality, with a relatively small effect in summer and a large effect in fall.

The AMO exerts a low-frequency modulation on the annual AWP area variance primarily through modulating ENSO and the local heat flux feedback, whereas the NAO teleconnection and ocean mixed layer depth play negative roles. ENSO amplitude becomes small (large) during the AMO warm (cold) phase, which is largely due to a change of the mean state. When the AMO is in its warm (cold) phase, the tropical Pacific thermocline becomes deep (shallow),

which in turn leads to a small (large) amplitude of ENSO. Mechanisms of the AMO-induced thermocline change in the tropical Pacific may be associated with both ocean and atmospheric bridges (Timmermann et al. 2005; Sutton and Hodson 2006). The AMO-modulated ENSO variability can ultimately teleconnect to the AWP region (Enfield and Mayer 1997; Klein et al. 1999). Meanwhile, we find that the AMO-modulated seasonal cycle in the tropical Pacific also contributes to the multidecadal variation of ENSO amplitude due to the nonlinear interaction (Timmermann et al. 2007). Moreover, the local heat flux feedback is found to be strengthened during the AMO warm phase compared to that during the AMO cold phase. This induces a small (large) AWP area variance during the AMO warm (cold) phase. On the other hand, the modulations from ENSO teleconnection and the local heat flux feedback are countered by both the ocean mixed layer depth and the NAO. It is found that the ocean mixed layer depth tends to become shallow during the AMO warm phase, which favors a large AWP area variance. Similarly, the AMO-modulated NAO amplitude shows a large value during the AMO warm phase and a small value during the AMO cold phase.

Although ENSO teleconnection can explain the AMO-modulated AWP area variance, it can not completely determine its seasonality. The seasonality of the AWP area variance modulated by the AMO is also dominated by the local heat flux feedback and ocean mixed layer depth, and countered by the NAO teleconnection. It is shown that the negative heat flux feedback difference between the AMO warm and cold phases in fall is larger than that in summer, consistent with the seasonality of the modulated AWP area variance. Similarly, the ocean mixed layer depth shoals more in summer than that in fall, favoring a large AWP area variance during the AMO warm phase in summer. However, the AMO-modulated NAO amplitude exhibits a smaller value during the AMO warm phase than that during the AMO cold phase in summer and vice versa in fall, which is countered with the seasonality of AWP area variance modulated by the AMO.

The study here indicates that the AWP variability can be significantly modulated by the AMO. It is conceivable the assessing the predictability of the AWP variability should take into account low-frequency modulation from the AMO. An enhanced variability for the AWP area during the AMO cold phase may lead to a higher predictability of the AWP area variations. The results also further suggest to predict the AWP area variations, the coupled model perhaps should improve performance in capturing the AMO and its influences on both the NAO and ENSO.

**Acknowledgments** This work is supported by the National Creative Research Group Project (NSFC40921004), Scholarship Award for Excellent Doctoral Student granted by Ministry of Education and China National Natural Science Foundation Distinguished Young Investigator Project (40788002).

## References

Carton JA, Cao X, Giese BS, Silva AM (1996) Deacadal and interannual SST variability in the tropical Atlantic. J Phys Oceanogr 26:1165–1175

Chang P, Ji L, Li H (1997) A decadal climate variation in the tropical Atlantic Ocean from thermodynamic air–sea interactions. Nature 385:516–518

Chang P, Ji L, Saravanan R (2001) A hybrid coupled model study of tropical Atlantic variability. J Clim 14:361–390

Compo GP et al (2011) The twentieth century reanalysis project. Q J R Meteorol Soc 137:1–28

Covey DL, Hastenrath S (1978) The Pacific El Niño phenomenon and the Atlantic circulation. Mon Weather Rev 106:1280–1287

Curtis S, Hastenrath S (1995) Forcing of anomalous sea surface temperature evolution in the tropical Atlantic during Pacific warm events. J Geophys Res 100:15835–15847

Czaja A, Marshall J (2001) Observations of atmosphere–ocean coupling in the North Atlantic. Q J R Meteor Soc 127:1893–1916

Czaja A, Van der Vaart P, Marshall J (2002) A diagnostic study of the role of remote forcing in tropical Atlantic variability. J Geophys Res 15:3280–3290

Delworth TL, Mann ME (2000) Observed and simulated multidecadal variability in the Northern Hemisphere. Clim Dyn 16:661–676

Dong BR, Sutton T, Scaife AA (2006) Multidecadal modulation of El Niño–Southern Oscillation (ENSO) variance by Atlantic Ocean sea surface temperatures. Geophys Res Lett 33:L08705. doi: 10.1029/2006GL025766

Enfield DB, Mayer DA (1997) Tropical Atlantic sea surface temperature variability and its relation to El Niño-Southern oscillation. J Geophys Res 102:929–945

Enfield DB, Mestas-Nuñez AM (1999) Multiscale variabilities in global sea surface temperatures and their relationships with tropospheric climate patterns. J Clim 12:2719–2733

Enfield DB, Mestas-Nuñez AM, Trimble PJ (2001) The Atlantic multidecadal oscillation and its relation to rainfall and river flows in the continental US. Geophys Res Lett 28:2077–2080

Enfield DB, Lee SK, Wang C (2006) How are large western hemisphere warm pools formed? Prog Oceanogr 70:346–365

Enfield DB, Mestas-Nuñez AM, Mayer DA, Cid-Serrano L (1999) How ubiquitous is the dipole relationship in tropical Atlantic sea surface temperatures? J Geophys Res 104:7841–7848

Folland CK, Parker DE, Palmer TN (1986) Sahel rainfall and worldwide sea temperatures, 1901–85. Nature 320:602–607

Folland CK, Colman AW, Rowell DP, Davey MK (2001) Predictability of northeast Brazil rainfall and real-time forecast skill, 1987–98. J Clim 14:1937–1958

Frankignoul C, Kestenare E (2002) The surface heat flux feedback. Part I: estimates from observations in the Atlantic and the North Pacific. Clim Dyn 19:633–647

Giannini A, Kushnir Y, Cane MA (2000) Interannual variability of Caribbean rainfall, ENSO and the Atlantic Ocean. J Clim 13:297–311

Giannini A, Cane MA, Kushnir Y (2001) Interdecadal changes in the ENSO teleconnection to the Caribbean region and the North Atlantic Oscillation. J Clim 14:2867–2879

Goldenberg SB, Landsea CW, Mestas-Nuñez AM, Gray WM (2001) The recent increase in Atlantic hurricane activity: causes and implications. Science 293:474–479

Gray WM, Sheaffer JD, Landsea CW (1997) Climate trends associated with multidecadal variability of Atlantic hurricane activity. In: Diaz HF, Pulwarty RS (eds) Hurricanes: climate and socioeconomic impacts. Springer, New York, pp 15–53

Grotzner A, Latif M, Barnett TP (1998) A decadal climate cycle in the North Atlantic Ocean as simlulated by the ECHO coupled GCM. J Clim 11:831–847

Halliwell GR, Mayer DA (1996) Frequency response properties of forced climatic SST anomaly variability in the North Atlantic. J Clim 9:3575–3587

Hastenrath S (2000) Upper air mechanisms of the Southern Oscillation in the tropical Atlantic sector. J Geophys Res 105:14997–15009

Hastenrath S, Wu MC, Chu PS (1984) Toward the monitoring and prediction of north-east Brazil droughts. Q J R Meteorol Soc 110:411–425

Hastenrath S, de Castro LC, Aceituno P (1987) The southern oscillation in the Atlantic sector. Contribut Atmos Phys 60:447–463

Horel JD, Wallace JM (1981) Planetary-scale atmospheric phenomena associated with the Southern Oscillation. Mon Weather Rev 109:813–829

Hoskins BJ, Karoly K (1981) The steady response of a spherical atmosphere to thermal and orographic forcing. J Atmos Sci 38:1179–1196

Houghton RW, Tourre YM (1992) Characteristics of low-frequency sea surface temperature fluctuations in the tropical Atlantic. J Clim 5:765–771

Kerr RA (2000) A North Atlantic pacemaker for the centuries. Science 288:1984–1986

Klein SA, Soden BJ, Lau NC (1999) Remote sea surface temperature variations during ENSO: evidence for a tropical atmospheric bridge. J Clim 12:917–932

Knight JR, Allan RJ, Folland CK, Vellinga M, Mann ME (2005) A signature of persistent natural thermohaline circulation cycles in observed climate. Geophys Res Lett 32:L20708. doi: 10.1029/2005GL024233

McCabe GJ, Palecki MA, Betancourt JL (2004) Pacific and Atlantic Ocean influences on multidecadal drought frequency in the United States. Proc Natl Acad Sci 101:4136–4141

Mestas-Nuñez AM, Enfield DB (1999) Rotated global modes of non-ENSO sea surface temperature variability. J Clim 12:2734–2746

Mo KC, Häkkinen S (2001) Interannual variability in the tropical Atlantic and linkages to the Pacific. J Clim 14:2740–2762

Nigam S (2003) Teleconnections. In: Holton JR, Pyle JA, Curry JA (eds) Encyclopedia of Atmospheric Sciences. Academic Press, London, pp 2243–2269

Rayner N, Parker DE, Horton EB, Folland CK, Alexander LV, Rowell DP, Kent EC, Kaplan A (2003) Global analyses of sea surface temperature, sea ice, and night marine air temperature since the late nineteenth century. J Geophys Res 108:4407. doi: 10.1029/2002JD002670

Rowell DP (2003) The impact of Mediterranean SSTs on the Sahelian rainfall season. J Clim 16:849–862

Rowell DP, Folland CK, Maskell K, Ward MN (1995) Variability of summer rainfall over tropical North-Africa (1906–92) observations and modelling. Q J R Meteorol Soc 121:669–704

Saravanan R, Chang P (2000) Interaction between tropical Atlantic variability and El Niño-Southern Oscillation. J Clim 13:2177–2194

Schlesinger ME, Ramankutty N (1994) An oscillation in the global climate system of period 65–70 years. Nature 367:723–726

Smith TM, Reynolds RW (2004) Improved extended reconstruction of SST (1854–1997). J Clim 17:2466–2477

Sutton RT, Hodson DLR (2005) Atlantic Ocean forcing of North American and European summer climate. Science 309:115–118

Sutton RT, Hodson DLR (2006) Climate response to multidecadal warming and cooling of the North Atlantic Ocean. J Clim (submitted)

Timmermann A, An SI, Krebs U, Goosse H (2005) ENSO suppression due to weakening of the North Atlantic thermohaline circulation. J Clim 18:3122–3139

Timmermann A, Lorenz S, An SI, Clement A, Xie SP (2007) The effect of orbital forcing on the mean climate and variability of the tropical Pacific. J Clim 20:4147–4159

Wang C (2002) Atmospheric circulation cells associated with the El Niño-Southern oscillation. J Clim 15:399–419

Wang C, Enfield DB (2001) The tropical Western Hemisphere warm pool. Geophys Res Lett 28:1635–1638

Wang C, Enfield DB (2003) A further study of the tropical Western Hemisphere warm pool. J Clim 16:1476–1493

Wang C, Enfield DB, Lee SK, Landsea CW (2006) Influences of the Atlantic warm pool on Western Hemisphere summer rainfall and Atlantic hurricanes. J Clim 19:3011–3028

Wang C, Lee SK, Enfield DB (2008a) Climate response to anomalously large and small Atlantic warm pools during the summer. J Clim 21:2437–2450

Wang C, Lee SK, Enfield DB (2008b) Atlantic warm pool acting as a link between Atlantic multidecadal oscillation and Atlantic tropical cyclone activity. Geochem Geophys Geosyst 9 Q05V03. doi: 10.1029/2007GC001809

Xie SP, Philander SGH (1994) A coupled ocean–atmosphere model of relevance to the ITCZ in the eastern Pacific. Tellus 46:340–350